A Long-Range Dynamic GPS Processing System for Aircraft Navigation and Positioning

Yanming Feng & Kurt Kubik, Queensland University of Technology, Australia
Shaowei Han, The University of New South Wales, Sydney, Australia

WG I/2 - System Aspects of Platform Guidance, Navigation and Sensor Positioning

KEY WORDS: GPS, real time dynamic positioning, Kalman filtering and smoothing, aircraft navigation and positioning.

ABSTRACT

On-The-Fly integer ambiguity resolution for long-range dynamic or kinematic GPS positioning is difficult to achieve. As a result, although quite a large number of originations have established their own versions of On-The-Fly software which has been very promising for short-range positioning, none has been successfully developed for long range dynamic GPS navigation and positioning. The paper documents a dynamic GPS processing prototype system that achieves decimetre-level accuracy in real time and 1ppm accuracy off-line (by postprocessing) in three dimensions over the range of a few hundred kilometres without OTF ambiguity resolutions. The prototype system was based on two important strategies. Firstly, it detects and removes any carrier phase cycle slips between two epochs in which there may be a data gap of a few seconds to a few minutes, depending on the user's receivers and user's environments. Secondly, phase delta-positions and DGPS code positions are obtained without the needs of resolving ambiguities, which are then reprocessed in real time by Kalman filtering approaches to achieving decimetre accuracy, and off line by Kalman smoothing techniques for achieving 1ppm accuracy in three dimensions. This paper describes the theoretical basis of the developed long range dynamic GPS positioning system and gives experimental results for aircraft and navigation positioning, which confirm the achievable cycle-slip detectability and positioning capability.

1. INTRODUCTION

Much research has been done into fast and efficient ways to resolve carrier phase ambiguities, in order to enable GPS users to realise the maximum potential accuracy of GPS carrier phase measurements. As a result, many organisations have developed their own versions of kinematic GPS positioning software (Deloach et al, 1995), the majority of which is based on the so-called On-The-Fly (OTF) ambiguity resolution technique. OTF techniques promise real - time centimetre positioning in three dimensions. However, almost all the existing systems were designed for short-range kinematic (or dynamic) positioning environments, and none has so far been successfully developed for long-range dynamic applications. There are two major reasons for this. The first reason is that for long-range dynamic or kinematic positioning, the integer ambiguity resolution is difficult to achieve from both ionosphere-free and ionosphere biased carrier phase measurements. The ionosphere-free combination of L1 and L2 carrier phase measurements has the wavelength of a few millimetres; any other combinations of L1 and L2 suffer from the ionospheric effects. Thus integer ambiguities can generally not be estimated in real time by the state-of the-art OTF techniques. The second reason is that the orbital errors and un-modelled troposphere effects on double difference carrier phase measurements increase as the distance between base and rover receivers increases (Chen, 1994). These errors make integer removal of cycle-slips or integer searching of ambiguity resolutions on the fly over lang ranges more difficult and even impossible. Thus, centimetre accuracy is difficult to achieve for long range applications.

However, for aircraft guidance, navigation and sensor positioning for photogrammetry, real time decimetre accuracy and 1ppm accuracy off line in three dimensions over the range from a few tens to hundreds kilometres may be quite acceptable. This may be achieved in theory without On The Fly ambiguity resolutions (Feng, 1995; Cannon, 1995). On the other hand, the use of dual frequency carrier phase observable also makes it possible to detect and repair cycle slips depending on carrier phase measurements (Hofmann 1992; Han, 1995) rather than On-The-Fly techniques, which allow integer ambiguities to be resolved again for kinematic process over short-ranges when a cycle slip occurs. Our strategy for long-range kinematic or dynamic positioning is therefore to remove cycle slips and realise decimetre accuracy in real time not depending on OTF ambiguity resolutions.

The development of a long range dynamic (LRD) GPS positioning system aims to provide a prototype system capable of decimetre positioning in real time and 1ppm accuracy by postprocessing. This paper addresses the theoretical basis for the LRD system and experimental results. Firstly, a method for cycle-slip detection and cycle-slip repair after data gaps are proposed, based on L1/L2 and P-code measurements. This is followed by a method which jointly uses the code and phase measurements to create delta-positions and position sequences. These results are

then further processed on line (real time) for achieving decimetre accuracy positioning and 1ppm accuracy by postprocessing. Finally experimental results for aircraft positioning are given, which confirm the achievable decimetre-level positioning capability

2. DETECTION AND REPAIR OF CARRIER PHASE CYCLE SLIPS

We assume the use of dual frequency GPS receivers with C/A code and/or P code pseudorange measurements. Thus, there are four possible observation equations (Dong & Bock, 1989):

$$R_1 = \rho + I/f_1^2 + \varepsilon_{R1} \quad (1)$$
$$\varphi_1\lambda_1 = \rho - I/f_1^2 + \lambda_1 N_1 + \varepsilon_{\varphi 1} \quad (2)$$
$$R_2 = \rho + I/f_2^2 + \varepsilon_{R2} \quad (3)$$
$$\varphi_2\lambda_2 = \rho - I/f_2^2 + \lambda_2 N_2 + \varepsilon_{\varphi 2} \quad (4)$$

where R_1 is C/A code or P1 code pseudorange, and R_2 is P2 code pseudorange; φ_1 and φ_2 are the L1 and L2 carrier phase measurements in units of cycles whose frequencies are f_1 and f_2 and wavelengths λ_1 and λ_2, N_1 and N_2 denote integer cycle ambiguities, ρ is the geometric range of the receiver to a satellite; I is defined by Total Electron Content (TEC) and ε denotes the noise in the various measurements.

The linear combination of φ_1 and φ_2 creates a new observable (Han & Rizos, 1995)

$$\varphi_{i,j} = i\,\varphi_1 + j\,\varphi_2 \quad (5)$$

where i,j denote arbitrary integers. Its integer ambiguity and wavelength are

$$N_{i,j} = i\,N_1 + j\,N_2 \quad (6)$$
$$\lambda_{i,j} = c/(i\,f_1 + j\,f_2) \quad (7)$$

where c is the speed of the light. According to the equations 1-4, the real-valued ambiguity $N_{i,j}$ for the combined phase $\varphi_{i,j}$ can be written as:

$$N_{i,j} = \varphi_{i,j} - \alpha_1 R_1 + \alpha_2 R_2 \quad (8a)$$

where

$$\alpha_1 = [\,9240(i+j) + 289\,i\,] / 2329\lambda_1 \quad (8b)$$
$$\alpha_2 = [\,9240(i+j) + 289\,j\,] / 2329\lambda_2 \quad (8c)$$

Formula (8) is designed for those cases where C/A code or P1-code and P2 -code pseudorange measurements are available. Studies have shown its good suitability for widelane ambiguity estimation (i=1,j=-1), but it is inaccurate for other phase combinations (Han & Rizos, 1995). Therefore, the following ionosphere-biased formula is considered as an alternative:

$$N_{i,j} = \varphi_{i,j} - R/\lambda_{i,j} + \gamma_{i,j}\,(I/f_1^2) \quad (9)$$

where

$$\gamma_{i,j} = (\alpha_{i,j} + \beta)/\lambda_{i,j} \quad (10a)$$
$$\alpha_{i,j} = (4620\cdot i + 5929\,j)/(4620\,i + 3600\,j) \quad (10b)$$
$$\beta = \begin{cases} 1.00 & \text{for } R = R_1 \\ 1.647 & \text{for } R = R_2 \\ 1.323 & \text{for } R = (R_1 + R_2)/2 \end{cases} \quad (10c)$$

R stands for R_1 or R_2 or the average of R_1 and R_2, depending on the measurements available.

Now, we wish to select some linear combinations of φ_1 and φ_2 for cycle slip detection and repair. In principle, the combinations which have 10 and 100 times of the L1 or L2 wavelengths would be considered as the most appropriate ones. The second factor is the noise of a combined phase ambiguity $N_{i,j}$ to be computed by Eq (8) or (9). The smaller the noise of the combined ambiguity and the larger its wavelength, the better the capacity of identifying the combined cycle slips. The third factor is the effect of the time-varying ionosphere biases on the determination of the combined ambiguity $N_{i,j}$. Table 1 gives the standard deviation (STD or 1σ error) estimates of several typical combined ambiguities $N_{i,j}$ and their coefficient $\gamma_{i,j}$, of the time-varying ionospheric biases, where $\varphi_{77,-60}$ is the ionosphere-free phase observable. It is noted that the maximum wavelength for possible L1 and L2 combinations is 14.653 metres, achieved by $\varphi_{-7,9}$. Considering all the three factors, the best possible choice for cycle slip detection is to use the combinations $N_{1,-1}$, defined by Eq (8) or Eq (9) and $N_{-7,9}$, defined by Eq (9).

Table 1 STDs for determining combined ambiguities

Phase	λ(m)	σ(cy)-Eq(8)	σ(cy) Eq(9)	γ-Eq (10) ($R=R_1$)
φ_1	.190	8.085	1.579	10.510
φ_2	.244	8.024	1.220	10.839
$\varphi_{77,-60}$	.006	142.02	47.679	158.948
$\varphi_{1,-1}$	.862	0.248	0.348	-0.329
$\varphi_{1,-2}$	.341	7.971	0.862	-11.167
$\varphi_{-3,4}$	1.682	7.886	0.191	11.825
$\varphi_{-7,9}$	14.653	15.740	0.116	23.979
Note: Assumptions for STD computations: $\sigma_{\varphi 1} = \sigma_{\varphi} = 0.01$ cycles, $\sigma_{R1} = \sigma_{R2} = 0.3$ metres				

The detectability of the cycle slips then depends on the temporal and spatial predictability of the ionosphere biases in Eq (9). Over a period of up to a few minutes, the regular variation of ionosphere biases can be represented as a linear function of time. This implies that a linear model of $N_{i,j}$, estimated from the observations within a moving time window in the past, can be used to predict the $N_{i,j}$ values at the next epoch. Using the predicted value $N_{i,j}$ (k, k-1) and observation value $N_{i,j}$(k) at the epoch k, the differences $DN_{i,j}$(k) are obtained to detect and repair the cycle slips at this epoch:

$$DN_{1,-1}(k) = N_{1,-1}(k) - N_{1,-1}(k, k-1) \quad (13)$$
$$DN_{-7,9}(k) = N_{-7,9}(k) - N_{-7,9}(k,k-1) \quad (14)$$

This principle can also be used to estimate cycle slips which may have occurred during data gaps, that is during periods where no navigation solution was possible (due to shielding a.o.). It is difficult to determine the maximum allowable length of these data gaps as the noise and ionosphere irregularity and scintillation as well the multipath effects accumulate with prediction time. In practice, the valid predictable time may be identified through data analysis of observation sequences.

After determining the integer cycle slips of $DN_{1,-1}$ and $DN_{-7,9}$, denoted by $CS_{1,-1}$ and $CS_{-7,9}$, the cycle slips CS_1 and CS_2 of φ_1 and φ_2 are finally determined by the following relations:

$$CS_1 = (CS_{-7,9} + 9\, CS_{1,-1}) / 2 \quad (15)$$
$$CS_2 = (CS_{-7,9} + 7\, CS_{1,-1}) / 2 \quad (16)$$

This procedure does not necessarily produce unique integer solutions but integer candidates for cycle slips of each combination because of the error accumulation with the growth of data gaps and existence of code biases and multipath. In order to determine unique integer candidates without on the fly ambiguity resolution, it is referred to the test procedure proposed by Han (1995), which consists of a normality and two Fisher tests and has been proven very efficient for different dynamic environments.

3. DYNAMIC FILTERING AND SMOOTHING FOR CODE AND PHASE SOLUTIONS

The main feature of this method is to use delta-position solutions of first-order phase differences between epochs to filter and smooth the position solutions of psuedorange measurements. The process includes three steps: first, the double differenced ionosphere-free phase and pseudorange measurements are used to create the delta position and positions in three dimensions in real time (on-line); second, a on-line Kalman filter is designed to improve the positions with delta-position solution from metre-level accuracy to decimetre in real time, and third, optimal smoothing is performed off-line for achieving better position accuracy.

3.1 Phase delta-position and code position solutions

Precise delta coordinates of the rover receiver can be computed from the double differenced ionosphere-free phase measurements as follows:

$$\Delta\nabla\varphi_{77,-60}(k) = \Delta\nabla\,\rho(k) + \lambda_{77,-60}\,\Delta\nabla\,N_{77,-60} + \Delta\nabla\varepsilon_{\varphi} \quad (17)$$

where k denotes the time epoch. Differencing the equations for epochs k+1, and k, we have

$$\delta\Delta\nabla\varphi_{77,-60}(k+1) = \Delta\nabla\,\rho(k+1) - \Delta\nabla\,\rho(k) + \delta\Delta\nabla\varepsilon_{\varphi}(k+1) \quad (18)$$

where $\delta\Delta\nabla\varphi_{77,-60}(k+1) = \Delta\nabla\varphi_{77,-60}(k+1) - \Delta\nabla\varphi_{77,-60}(k)$. The equation for double differenced ionosphere-free code measurements is

$$\Delta\nabla R_c(k+1) = \Delta\nabla\,\rho(k+1) + \Delta\nabla\varepsilon_R(k+1) \quad (19)$$

where R_c stands for ionosphere-free pseudorange measurements. Linearising the equations (18) and (19) leads to

$$\delta\Delta\nabla\varphi_{77,-60}(k+1) = [\partial(\Delta\nabla\rho(k))/\partial X(k)]\delta X(k+1,k) + [\partial\Delta\nabla\rho(k+1)/\partial X(k+1) - \partial(\Delta\nabla\rho(k))/\partial X(k)]\,\delta X(k+1) + [\Delta\nabla\rho^0(k+1) - \Delta\nabla\rho^0(k)] + \delta\Delta\nabla\varepsilon_{\varphi}(k+1) \quad (20)$$

$$\Delta\nabla R_c(k+1) = [\partial(\Delta\nabla\rho(k+1))/\partial X(k+1)]\delta X(k+1) + \Delta\nabla\,\rho^0(k+1) + \Delta\nabla\varepsilon_R(k+1) \quad (21)$$

where $\delta X(k+1,k) = \delta X(k+1) - \delta X(k)$ denotes the delta position vector between the epoch k+1 and k. The value $\rho^0(k)$ is computed from approximate coordinate vector $X^0(k)$. A minimum of four visible satellites is required to form three equations for both types of code and phase measurements. Thus, the least square solutions of both $\delta X(k+1,k)$ and $\delta X(k+1)$ can be obtained by the joint use of those two equations. It is noticed that this is a quite loose combination as the coefficient of $\delta X(k+1)$ are and there is a significant difference between carrier phase noise and code ranging noise. The former is normally in the level of millimetre to centimetres and the latter is in the order of metres to tens of metres, depending on the user receivers and environments.

3.2 Optimal Filtering Of Phase Delta-Position And Code Position Solutions

The following filter algorithm is applied in order to achieve decimetre accuracy of the position solution. The filter equations consist of a set of state equation and vector observations

$$\mathbf{z}(k) = \Phi(k,k-1)\mathbf{z}(k-1) + w(k-1) \quad (22)$$
$$y(k) = A(k)\,\mathbf{z}(k) + \varepsilon(k) \quad (23)$$

where $\mathbf{z}(k)$ is the 6x1 state vector consisting of the 3x1 position vector $\mathbf{x}$ and the 3x1 velocity vector $\mathbf{v}$, y(k) is a 6x1

observation vector , containing the code position solution $X(k) = \delta X(k)+X^0(k)$ and delta position solution $X(k,k-1) =\delta X(k,k-1)+X^0(k,k-1)$.The matrix Φ is a 6x6 state transition matrix and A is the 6x6 observation matrix; w(k) is the 6x1 dynamic noise vector and $\varepsilon(k)$ is the noise vectors of X(k) and X(k,k-1). The Kalman filtering solutions to this system can be written as

$$\hat{\mathbf{z}}(k)=\Phi(k,k-1)\,\hat{\mathbf{z}}(k-1)+K(k)[y(k)-A(k)\,\Phi(k,k-1)\,\hat{\mathbf{z}}(k-1)] \quad (24)$$

where

$$K(k)= D(k)\,A^T(k)\,P^{-1}(k) \quad (25)$$

$$D(k)= [D^{-1}(k,k-1) + A^T(k)P^{-1}(k)\,A(k)\,]^{-1} \quad (26)$$

$$D(k,k-1)= \Phi(k,k-1)D(k-1)\Phi^T(k,k-1) + Q(k-1) \quad (27)$$

P(k) and Q(k) are the variance matrices for observation noise and dynamic noise. If the dynamic noise and phase delta position noise are negligible, comparing to the code position noise, the Kalman filtering solution of the 3 dimensional position state vector x can be simplified to

$$\hat{\mathbf{x}}(k)=D_x(k)\{D_x^{-1}(k-1)[\,\hat{\mathbf{x}}(k-1)+ X(k,k-1)]+ P_x^{-1}(k)\,X(k)\} \quad (28)$$

$$D_x(k)=[D_x^{-1}(k-1) + P_x^{-1}(k)]^{-1} \quad (29)$$

where P_x stands for the variance matrix of code position solution X(k). and D_x denotes the filtering variance matrix of the position state vector; $D_x^{-1}(0) =0$ is assumed for k=1.

If the errors of different position components are assumed to be mutually independent and identical in accuracy, the equations (28) and (29) partition into the three estimates of the individual coordinate components:

$$\hat{\mathbf{x}}_m(k)=\{(k-1)[\,\hat{\mathbf{x}}_m(k-1) + X_m(k,k-1)] +X_m(k)\}/k \quad (30)$$

where the subscript m denotes three position components latitude, longitude and height or x, y and z when m=1,2, 3.

3.3 Optimal Smoothing of Phase Delta-Position and Code Position Solutions

Optimal Kalman filtering uses all the to-date measurements to create the position state vector solutions in real time mode. Kalman smoothing, however allows us to utilise all the measurements for achieving uniformly accurate solutions in postprocessing mode. As the optimal smoothing equations for the system equations (22) and (23) can be found in related textbooks, only a simplified formula is given here, based on the assumption that the dynamic noise and delta-position noise can be ignored with respect to code position noise. Therefore, the smoothing position vector is written as

$$\hat{\mathbf{x}}(j) = D_x^n\,\Sigma_{k=1}^n\,[X(k)+ X(j,k)]\,P_x^{-1}(k) \quad (31)$$

where

$$D_x^n = [\Sigma_{k=1}^n\,P_x^{-1}(k)]^{-1} \quad (32)$$

$$X(j,k)= X(k+1,k)+ X(k+2,k+1) + \ldots X(j,j-1) \quad (33)$$

where $X(k,k)=0$ and $X(k,j)= -X(j,k)$ are assumed. Similarly, if the errors of different position components are assumed to be mutually independent and identical in accuracy, the equations (31) and (32) partition into the three estimates of the individual coordinate components:

$$\hat{\mathbf{x}}_m(j) = \Sigma_{k=1}^n\,[\,X_m(k) + X_m(j,k)]\,/n \quad (34)$$

where n is the cumulative tracking time in epochs, and j=1, 2,..., n

3.4 Asymptotical Performance of Dynamic Filtering and Smoothing Solutions

Because the linear system of (22) and (23) is uniformly, completely observable and uniformly, completely controllable, its Kalman filtering solutions are uniformly, asymptotically stable (Feng & Kubik, 1994). In other words, the position solution converges to an asymptotic level of accuracy with increasing tracking time: The longer the continuous tracking time, the more accurate the state filtering solution will be. According to the equations (30) and (34), and assuming random noise, the variance of the filtering solution $\hat{\mathbf{x}}(k)$ and the smoothing solution $\hat{\mathbf{x}}(j)$ can be approximately estimated as

$$\sigma^2_{\hat{x}m}(k) = \sigma^2 / k \quad (35)$$

$$\sigma^2_{\hat{x}m}(j) = \sigma^2 / n \quad (36)$$

where σ^2 denotes the variance of code position solution X, and $\sigma^2_{\hat{x}m}(k)$ and $\sigma^2_{\hat{x}m}(j)$ denote the variances of filtering solution $\hat{\mathbf{x}}_m(k)$. and smoothing solution $\hat{\mathbf{x}}_m(j)$. It can be seen that the smoothing solutions are uniformly accurate while the filtering solutions are asymptotically stable. This asymptotical nature allows for the direct comparison between known baseline vector and the smoothing positions. Once the smoothing solutions are corrected to the known baseline, centimetre accuracy may be achievable.

Figure 1 shows the convergence of the filtering variance with filtering time and the effects of different noise levels of the code solutions onto this resulting accuracy. However, this theoretical accuracy model has only limited validity because both code position vector X(k) and delta- position vector X(k,k-1) are affected by systematic error sources such as un-modelled troposphere errors, GPS orbital errors and multipath. The magnitude of these effects depends on the user's receiver and the measurement environment.

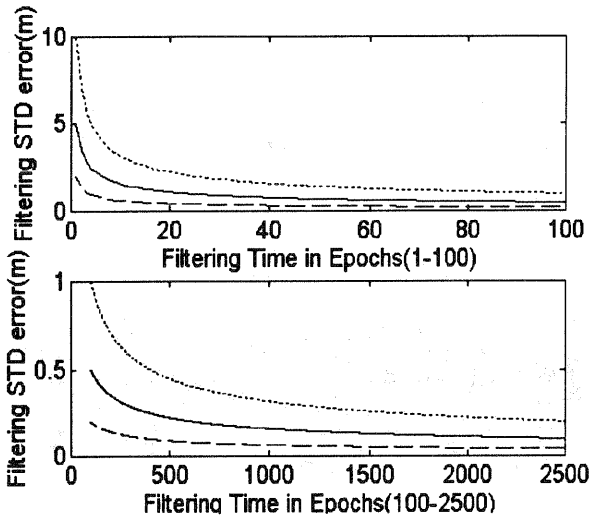

Figure 1 The Convergence of Filtering Accuracy with Time, where the standard deviations of the code position are assumed as 10 m (dot line), 5 m (solid line) and 2 m (broken line).

From this figure we learn that this method allows under good conditions for real-time positioning with decimetre accuracy or better. Also, the method is suitable for any ranges and dynamic environments as no assumptions where necessary relating to the baseline length and receiver's dynamics.

4. AIRBORNE TEST RESULTS AND ANALYSIS

4.1 Description Of The Long-Range Dynamic (LRD) GPS Processing System

The LRD system processes the measurements from both base and mobile receivers epoch by epoch. First, cycle slip detection and removal for one-way phase measurements is performed on the basis of combined phase measurements $N_{1,-1}$ and $N_{-7,9}$. Next, the accepted integer candidates are used to compute the residuals of ionosphere-free double difference measurements and then form a Fisher test statistic for selecting correct integer cycle slips (Han, 1995). After this, ionosphere-free double differenced phase and code ranges are jointly used to create delta-position vectors and position vectors, followed by the described on-line filtering and off-line smoothing processes, which require only 4 satellites for initialisation and maintenance and are therefore suitable for the environments with large mask angles; of course the use of more satellites are advantageous.

4.2 Testing Results For Cycle Slip Detection And Repair

Airborne DGPS kinematic data were collected on June 4 1992 from two Trimble Geodesist IIP GPS receivers. L1 and L2 carrier phase and C/A code and P2 code data were available for use. The base station was located some 57 meters from the take-off and touch-down site of the aeroplane. The data were logged every second for 2.5 hours, including static tracking periods of 4-5 minutes before take-off and after landing. Figure 1 shows the 2D trajectory of the aeroplane, whose height was 4500 metres during the en route phase of the flight. To demonstrate our method's efficiency for cycle slip detection and repair, the real-valued cycle estimates of $DN_{1,-1}$ and $DN_{-7,9}$ of PRN 23 for the airborne receiver are plotted in Figure 3a and b, where a moving time window of ten seconds of data was used to fit the ionosphere variation while the prediction time is set to one second. It can be seen that the noise of $DN_{-7,9}$ is normally bounded within the range of ±0.20cycles (1 cycle = 14.653m), thus the integer $CS_{-7,9}$ can be uniquely determined. The $DN_{1,-1}$ noise sometimes exceeds 0.5 cycle (1 cycle= .864m). The $CS_{1,-1}$ variable may therefore have two integer solutions, and the test procedure proposed in Han (1995) is applied to select an unique integer candidate. In order to test the method's ability for data gap removal, the prediction time was set to 60 seconds and the moving time window was set to 1 minute. Figure 4a,b show the real-valued cycle estimates of $DN_{1,-1}(k+60)$ and $DN_{-7,9}(k+60)$ for the same satellite. The figure shows the significant increase in the noise level of the DN(k+60) estimates. Also in this example, correct integer cycles have been determined by the same test procedure.

4.3 Experimental Results for the Filtering Solutions

Four types of positioning solutions were obtained: the phase delta-position solution, the code position solution, the filtered solution and smoothing solution. In addition, as the initial baseline vector has been determined by an external

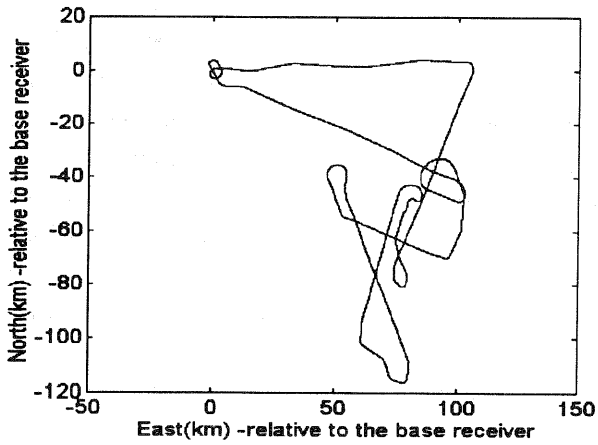

Figure 2 2D trajectory of the aeroplane, relative to the base receiver

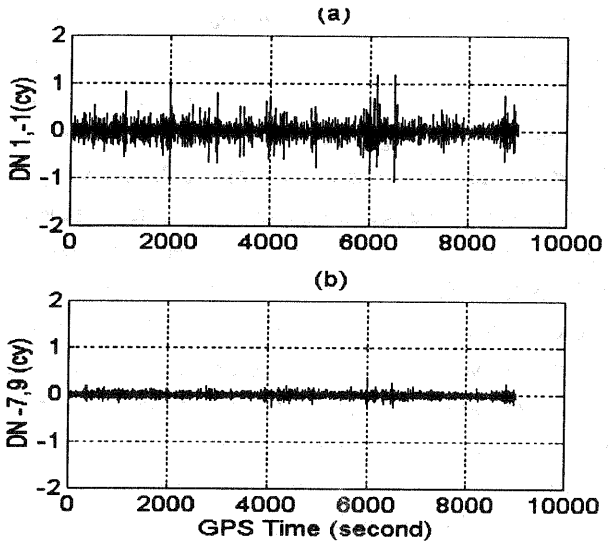

Figure 3. Real-valued estimates of the cycle slips, assuming data gaps of one second.

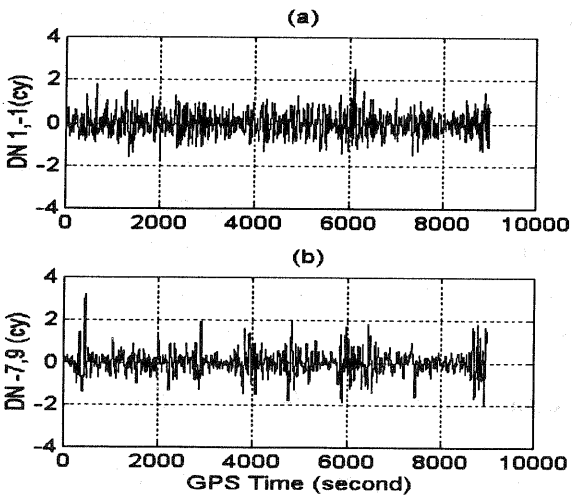

Figure 4. Real-valued estimates of the cycle slips, assuming data gaps of 60 seconds

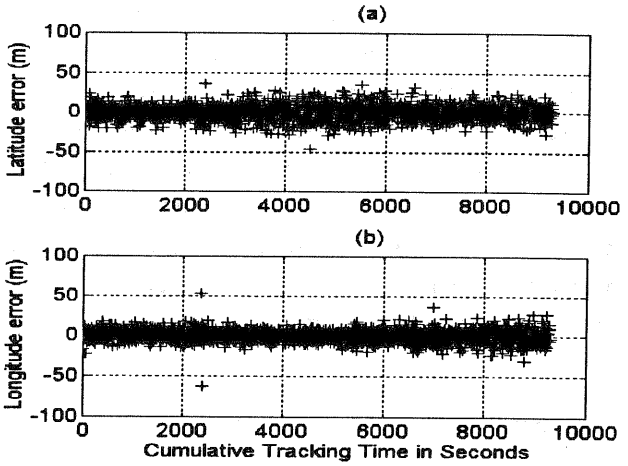

Figure 5. Deviations of code DGPS position solutions: (a) for the latitude component: σ=9.384m; and (b) for the longitude component: σ= 7.348m

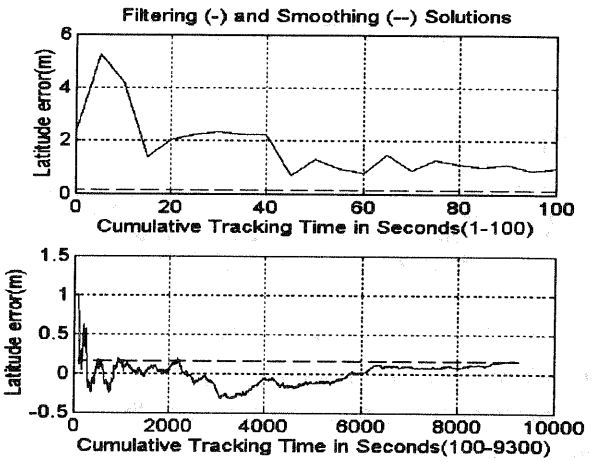

Figure 6. Convergence of the latitude filtering solutions with tracking time. Its standard deviation σ= 0.255m and the bias of smoothing solution: δ = +0.161m .

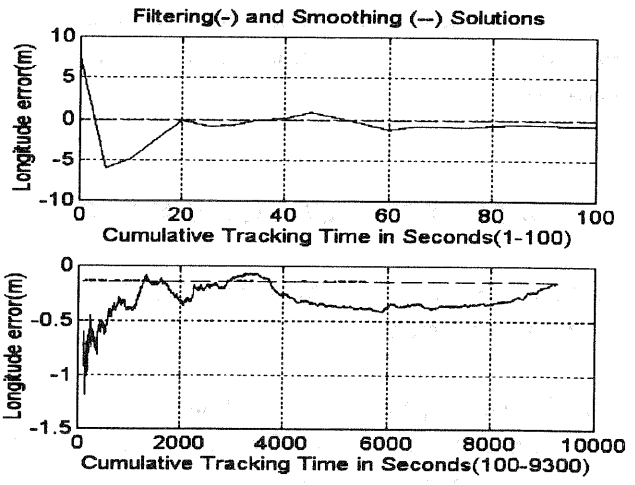

Figure 7. Convergence of the latitude filtering solutions with tracking time. Its standard deviation σ= 0.223m and the bias of smoothing solution: δ = -0.138m .

method, accurate to a couple of centimetres. This baseline can therefore be used together with the phase delta position solution to create a precise trajectory for validation of different LRD positioning solutions. Figure 5 show the differences between the precise trajectory and code DGPS position solutions of two horizontal components. It is noted that the noise of DGPS positioning solutions based on ionosphere-free pseudoranges is as high as tens of metres and the standard deviations for latitude and longitude components are 9.384m and 7.348m respectively. Comparing to the nominal figures of 2-5 metres for DGPS standard deviations, these STD values are considered quite high. Nevertheless, as shown in Figures 6 and 7, the accuracy of 20~30 centimetres in horizontal components can be achieved by the proposed filtering approach after about 10 minutes of the continuous tracking time. These figures clearly show the asymptotical stability of the filtering solutions. Not surprisingly, the figures also show the biases for the smoothing solution are -14 cm and 16 cm in latitude and longitude respectively, which may have been caused by the range-dependent systematic errors such as un-modelled troposphere biases and GPS broadcasting orbital errors as addressed previously.

5. CONCLUSIONS

Integer ambiguity resolution for long-range dynamic or kinematic positioning is difficult to achieve by using ionosphere-free carrier phase measurements. However, if the cycle slips and data gaps can be detected and removed successfully, the decimetre dynamic positioning may also be achieved without ambiguity resolutions. This is achieved by the long range dynamic GPS positioning method described in the paper. The method includes two strategies. First, it uses the phase combinations of $\varphi_{1,-1}$ and $\varphi_{-7,9}$ to detect and remove the cycle slips and short data gaps very efficiently. Secondly, it introduces Kalman filtering approach to the linear dynamic system to reprocess the phase-delta-position solutions and code position solution for achieving decimetre accuracy in real time. This requires on ambiguity resolution. The real time solutions are uniformly, asymptotically stable. The established particular LRD system is robust and reliable to use. The tests results have shown that the method for the detection and repair of cycle slips is efficient for the data gaps of up to 60 seconds for aircraft dynamic environment. Although the noise level of DGPS positioning solutions based on ionosphere-free pseudoranges reaches as high as tens of metres in this test, 20~30 centimetre accuracy in each component has been achieved by the proposed filtering approach. The smoothing solutions show the errors of -14 cm and 16 cm in latitude and longitude respectively, possibly due to range-dependent systematic errors such as un-modelled troposphere biases and GPS broadcasting orbital errors. In conclusion, the experimental results have confirmed the achievable decimetre accuracy on line (real-time) and off-line 1ppm accuracy of the proposed long range dynamic processing system.

REFERENCES

1. CHEN, D., Development of A fast Ambiguity Search Filtering (FASF) Method for GPS Carrier Phase Ambiguity Resolution, PhD Dissertation, The University of Calgary, 1994.
2. CANNON, E., Dynamic Real Time Precise Positioning, ION GPS -95 Tutorial, Palm Spring, September, 1995.
3. DELOACH, S.R, D. WELLS & D. DODD, Why On-the-Fly, GPS World, May, 1995.
4. DONG, D.N, & Y. BOCK, Global Positioning System network Analysis with Phase Ambiguity Resolution Applied to Crustal Deformation Studies in California, Journal of Geophysics, Vol 94, B4, 1989
5. FENG,Y.& KUBIK, On the internal stability of GPS Positioning Solutions, Submitted to Manuscripta Geodaetica, 1994.
6. FENG, Decimetre-Accuracy DGPS Achieved Without On-The-Fly Ambiguity Resolutions, Conference Proceedings of Satellite Navigation Technology: 1995 and Beyond, Brisbane, June 1995.
7. HAN, S. & C. RIZOS, A suggested procedure for On The Fly Ambiguity Resolution for long range Kinematic Positioning, Proceedings of 4th International Conference on Differential Satellite Navigation Systems, Bergen, Norway, April 1995.
8. HAN, S. Ambiguity Recovery fro Long Range Kinematic Positioning, The Proceedings of ION GPS 95, Palm Springs, September 1995.
9. HOFMANN-WELLENHOF, B., H.LICHTENEGGER, & J. COLLINS, GPS Theory and Practice, Springer-Verlag Wien New York, 1992